THE JOURNAL OF PHYSICAL CHEMISTRY Letters

Cite This: J. Phys. Chem. Lett. 2018, 9, 13−18

Letter

pubs.acs.org/JPCL

Coalescence-Induced Jumping of Nanodroplets on Textured Surfaces

Shan Gao, Quanwen Liao, Wei Liu,* and Zhichun Liu*

School of Energy and Power Engineering, Huazhong University of Science and Technology (HUST), Wuhan 430074, China

Supporting Information

ABSTRACT: Conducting experimental studies on nanoscale droplet coalescence using traditional microscopes is a challenging research topic, and views differ as to whether the spontaneous removal can occur in the coalescing nanodroplets. Here, a molecular dynamics simulation is carried out to investigate the coalescence process of two equally sized nanodroplets. On the basis of atomic coordinates, we compute the liquid bridge radii for various cases, which is described by a power law of spreading time, and these nanodroplets undergo coalescence in the inertially limited-viscous regime. Moreover, coalescence-induced jumping is also possible for the nanodroplets, and the attraction force between surface and water molecules plays a crucial role in this process, where the merged nanodroplets prefer to jump away from those surfaces with lower attraction force. When the solid−liquid interaction intensity and surface structure parameters are varied, the attraction force is shown to decrease with decreasing surface wettability intensity and solid fraction.

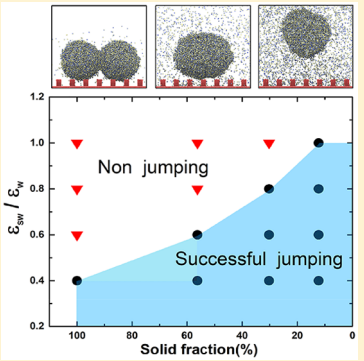

For a solid surface, it is well-known that its roughness and physicochemical properties can influence its wettability greatly. The contact angle of a water droplet on flat surfaces with low surface energy is generally 90°−120°, which is defined as a hydrophobic surface. However, for superhydrophobic surfaces, the value of contact angle can exceed 150° because of increased surface roughness of a hydrophobic surface.[1] Over the past decade, there have been several studies on the different aspects of superhydrophobic surfaces,[2−9] and promoting their unique properties has also been explored. Among these studies, the coalescence-induced jumping of water droplets, which was first reported by Boreyko and Chen on a superhydrophobic surface,[10] has recently received significant attention. This spontaneous droplet removal has been utilized for a variety of applications, including self-cleaning,[11] self-repelling,[12] anti-icing,[13] electrostatic energy harvesting,[14] and condensation heat-transfer enhancement.[15] Many researchers have conducted extensive studies on the jump motion of coalesced droplets, based on experiments,[16−21] theoretic analysis,[22,23] and simulations.[24,25] Nevertheless, according to the previous experimental observation, only those microdroplets coalescing on superhydrophobic surfaces can exhibit this self-propelled jumping. There are differing views on whether this spontaneous removal can happen to coalescing nanodroplets,[9,23,26−30] and its micromorphologic change and detailed mechanism are not well understood. It is challenging to conduct experimental research on the dynamic behavior of nanoscale droplets because of the limited spatial and time resolution of optical microscopes, and traditional macroscopic and mesoscopic simulation methods are not appropriate at the atomic scale. Conversely, molecular dynamics simulations can provide a powerful avenue to investigate the characteristics of droplets at the microscale level, without any assumption of the underlying continuum-level modeling.

In this Letter, molecular dynamics simulations were performed to study the evolution of two identical nanodroplets in the coalescence process on a series of surfaces with different solid fraction and wettability. During the initial coalescence stage, the liquid bridge radii for various cases are calculated and recorded. The radius is described as a power law of spreading time and is used to elucidate the inertially limited-viscous regime of these merged nanodroplets. Moreover, the findings show that coalescence-induced jumping is also possible in nanodroplets, which is ascribed to the low adhesion work between the surface and droplet. When the solid−liquid interaction intensity and surface structure parameters are varied, the attraction force is shown to decrease with decreasing surface wettability intensity and solid fraction, and the coalescence-induced jumping phenomenon preferentially occurs at those surfaces.

Schematic views of the simulation system are shown in Figure 1, where two static nanodroplets are placed very close to each other on the smooth substrate and the textured substrates. In order to improve the computation efficiency, more simple copperlike surfaces are used to simulate the real substrates with different surface energy (refer to the Supporting Information). To construct the nanodroplet and substrate, 33 514 water molecules and 127 400 copperlike atoms are used, respectively, both of which are initially generated in the face-centered cubic lattice, and the lattice constants of the unit cells are determined by each density at different temperatures. To acquire various degrees of surface wettability, the interaction energy well-depth, ε_W, between water molecules is fixed; the interaction energy well-depth, ε_{SW}, between substrate atoms and water molecules

Received: November 5, 2017
Accepted: December 13, 2017
Published: December 13, 2017

DOI: 10.1021/acs.jpclett.7b02939
J. Phys. Chem. Lett. 2018, 9, 13−18

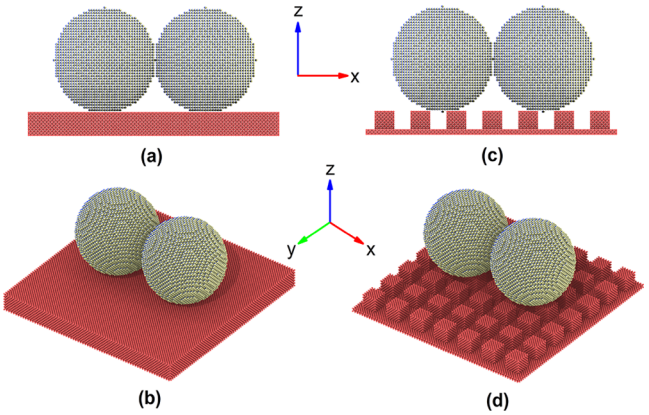

Figure 1. Initial configurations of two nanodroplets' coalescence on smooth substrate [(a) front view and (b) orthogonal view] and square pillared substrate [(c) front view and (d) orthogonal view].

is adjustable; and the energy parameter ratio, $\varepsilon_{SW}/\varepsilon_{W}$, represents surface wettability intensity, a detailed description of which is given in the Supporting Information. Textured substrates consist of a square pillar array with height H = 18.1 Å, different width W, and interpillar spacing S as detailed in Table 1. Gravity is not taken into consideration because the droplets are much smaller than the capillary length. The horizontal dimensions of all substrates correspond to 253.0 Å × 253.0 Å, and the spherical droplets have a fixed diameter of 100.7 Å. The properties of the droplet are taken to be the same as those of water at 20 °C, such that density ρ = 998.23 kg/m^3, surface tension σ = 72.75 mN/m, the liquid viscosity μ = 1.0087 mPa·s, and Ohnesorge number $Oh = \mu/\sqrt{\rho\sigma R}$, where R is the initial radius of droplet.

Table 1. Physical Dimensions of Pillars (Width, W; Distance between Pillars, S; and Height, H) and Structural Properties of Rough Surfaces (Solid Fraction $\phi_S = W^2/(W + S)^2$)

	S (Å)	W (Å)	H (Å)	ϕ_S (%)
structure 1	–	–	–	100
structure 2	9.04	27.11	18.1	56.24
structure 3	16.27	19.88	18.1	30.24
structure 4	23.49	12.65	18.1	12.25

In all subsequent simulations, there are 16 different types of surfaces established to study the effects of solid−liquid interaction intensity and solid fraction on nanodroplet coalescence. Typical coordinate snapshots of several cases are given in Figure 2, where the coalescence-induced jumping phenomenon took place only in those droplets on surfaces with certain wettability intensity and solid fraction; a specific analysis is provided in the following discussion. According to the time-lapse images, there are four stages in the coalescence-induced jumping process:[24] (I) formation and growth of the liquid bridge between two droplets; (II) impact of the liquid bridge on the surface; (III) reduction of the merged droplet's base area; (IV) upward motion of droplet, along with some oscillation. In order to illustrate the jumping process, the temporal vertical velocity of water molecules in the top contact region is plotted in Figure 2d. At the start of coalescence, because of the curvature difference between the liquid bridge radius and the droplet radius, Laplace pressure drives the liquid mass move to the center, leading to the expansion of the liquid bridge connecting the two droplets. At the beginning of stage II, the bottom liquid bridge has grown large enough to contact the surface, with a downward momentum. However, when the droplet interacts with the substrate, the downward-moving liquid mass is forced to move in reverse by the impermeable substrate. At stage III, the droplet moves upward and its base area reduces gradually, because the kinetic energy of the droplet is sufficient to overcome the adhesion work with the substrate. At stage IV, the departed droplet experiences deceleration due to the resistance originating from the collision between water molecules in the gas-phase region.

From the above diagram, we can clearly determine the evolution of the simulated interfacial shapes. At the beginning of the coalescence (stage I), a tiny liquid bridge forms and

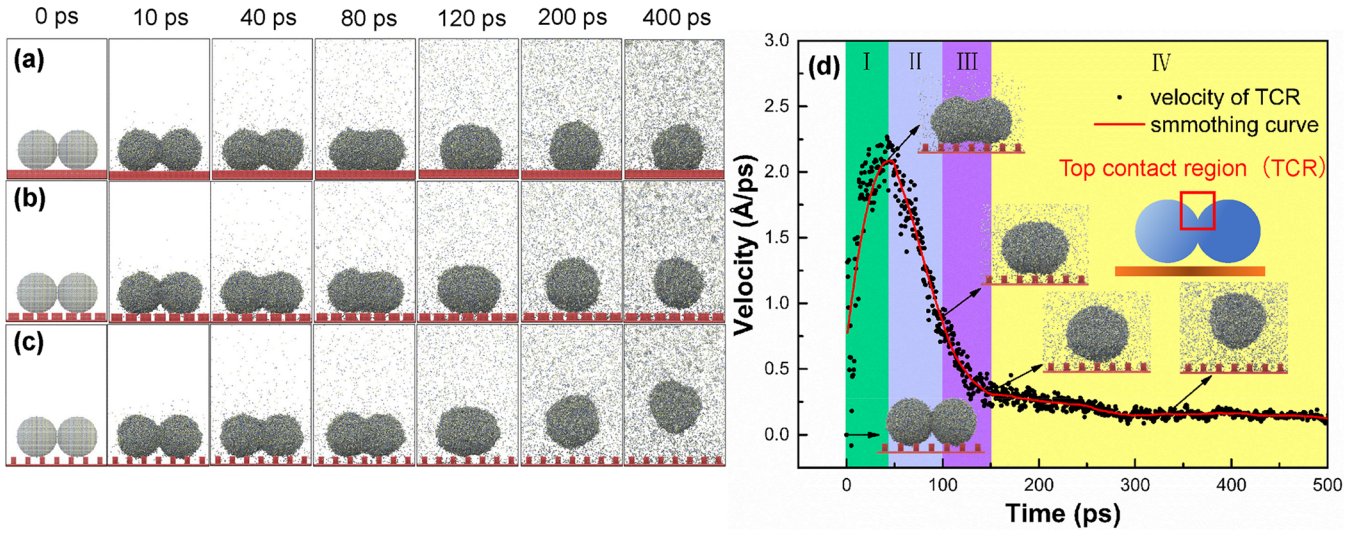

Figure 2. Time-lapse images of the coalescence process between two initially static nanodroplets. (a) A failed coalescence-induced jumping case (ϕ_S = 100%, $\varepsilon_{sw}/\varepsilon_{w}$ = 0.8). (b) A successful coalescence-induced jumping case (ϕ_S = 56.24%, $\varepsilon_{sw}/\varepsilon_{w}$ = 0.6). (c) A successful coalescence-induced jumping case (ϕ_S = 12.25%, $\varepsilon_{sw}/\varepsilon_{w}$ = 0.6). (d) Temporal evolution of the instantaneous vertical velocity in the top contact region. Insets illustrate the droplet morphology in these four specific stages.

DOI: 10.1021/acs.jpclett.7b02939
J. Phys. Chem. Lett. 2018, 9, 13−18

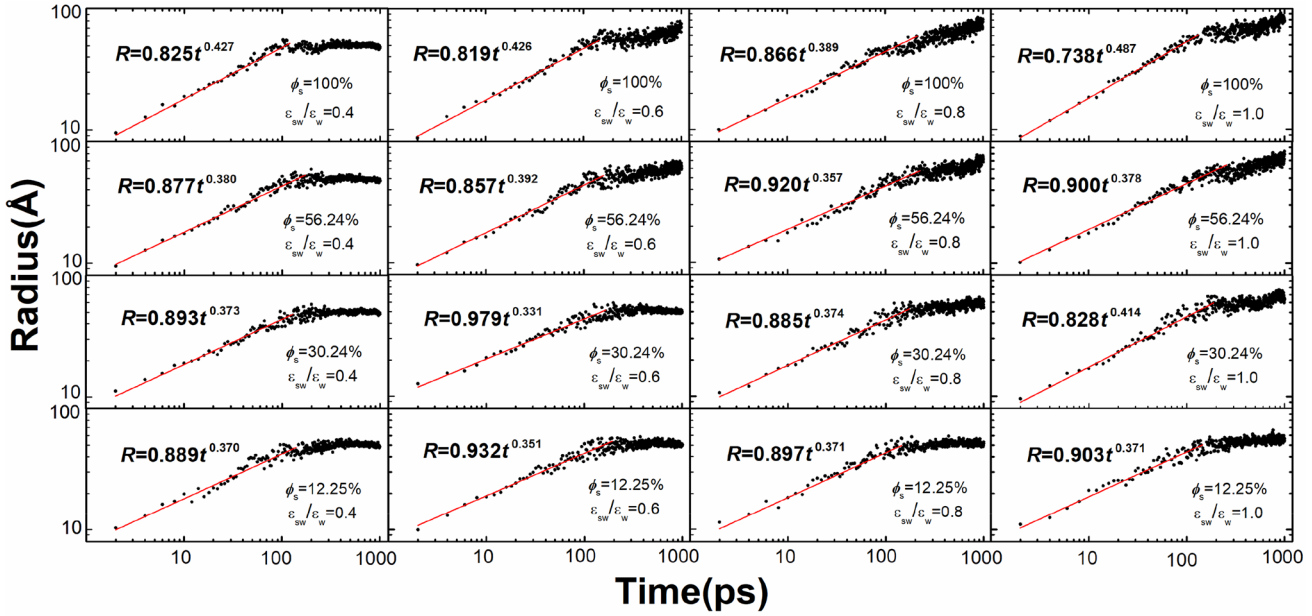

Figure 3. Liquid bridge radius as a function of time for all 16 cases. Black points denote the value of bridge radius, and the red line is a fit to the black points.

develops quickly, due to the large curvature difference between the bridge radius $(1/R_b)$ and the droplet radius $(1/R)$. The evolutionary pattern of the liquid bridge radius reflects which forces dominate in coalescence. Different regimes of coalescence have been studied,[31,32] and the mainstream understanding is that there are just two dynamical regimes of coalescence, with a crossover region between them: when $R_b/R < Oh$, the droplet undergoes coalescence in the viscous regime, then the inertial regime occurs at late times $(R_b/R > Oh)$ if viscous effects become negligible. Paulsen et al.[33] proposed a third new viewpoint, namely, inertially limited-viscous regime, where inertia and viscosity play a role in the dynamics. To determine the mechanism of nanodroplet coalescence in the inception stage, we recorded the variation of the liquid bridge radius with time for all cases, as shown in Figure 3. The function equations between liquid bridge radius and spreading time are obtained by linear fitting in a log−log coordinate. During the stage of liquid bridge expansion, its radius is expressed as the power law of spreading time, $R_b(t) \sim \alpha t^{\beta}$, and the values of prefactor α and exponent β are about 0.9 and 0.4, respectively. According to the phase diagram of coalescence, the relation of liquid bridge radius with time indicate that the nanodroplets undergo coalescence in the inertially limited-viscous regime.

For all the simulation cases, the results are presented in Figure 4a, where black points represent the successful jumping cases and red triangles represent the failed cases. To determine the relationship between merged droplets' behavior, surface wettability, and solid fraction, the centroid heights of droplets were extracted from the density contours of the processes, which are shown in Figure 4b, and the mass transfer between two droplets can be clearly observed. Figure 4c illustrates the effect of surface wettability on the evolution of droplets' centroid height by varying the energy parameter ratio $\varepsilon_{sw}/\varepsilon_w$ and keeping all other parameters fixed. The results show that the merged droplets can deviate from substrates more easily with decreasing surface wettability. Similarly, Figure 4d demonstrates the effect of the solid fraction on the evolution of droplets' centroid height; as the solid fraction decreases, there is an easily induced jumping for the merged droplets. Afterward, the droplets' centroid velocity is calculated based on the results of the droplets' centroid height, as shown in Figure 4e,f. In order to obtain the jumping velocities for all successful jumping cases, we compute the average values of centroid velocities within 50 ps of the jumping moment, as shown in Figure 4g, which illustrates that the jumping velocity decreases with increasing solid fraction and surface wettability approximately. For all jumping cases, the jumping velocities range from 0.05423 Å/ps to 0.12449 Å/ps; correspondingly, the calculated energy conversion efficiency is 0.15% ∼ 0.79%, a detailed description of which is given in the Supporting Information. The above results indicate that coalescence-induced jumping occurs preferentially on surfaces with lower surface wettability and solid fraction, so there is a forecast in Figure 4a where the blue shaded area represents all successful jumping cases. To confirm this conjecture, we calculated the attraction force between droplets and substrates for all cases. In addition, the relationships between the attraction force, surface wettability, and solid fraction were analyzed. Figure 5a shows the equipotential curve of interaction force between water molecules and substrates in the same unit area, where there exists a repulsive force and attractive force successively along the z axis direction. The work of adhesion is considered to play a role throughout the coalescence process, which is mainly herein associated with the attraction between water molecules and substrates,[24] because the droplet does not penetrate the structures in surfaces. The summation of attraction force in this unit area was calculated and is recorded in Figure 5b, where the attraction force decreases with the decreasing solid fraction and intensity of surface wettability. According to the results and analyses above, in those cases with low attraction force, the merged droplets can jump away from the surface because of the low adhesion work. The attraction force between surface and water molecules is crucial to the coalescence-induced jumping, and furthermore, the surface wettability and solid fraction play a remarkable role in the adjustment of the attraction force.

DOI: 10.1021/acs.jpclett.7b02939
J. Phys. Chem. Lett. 2018, 9, 13−18

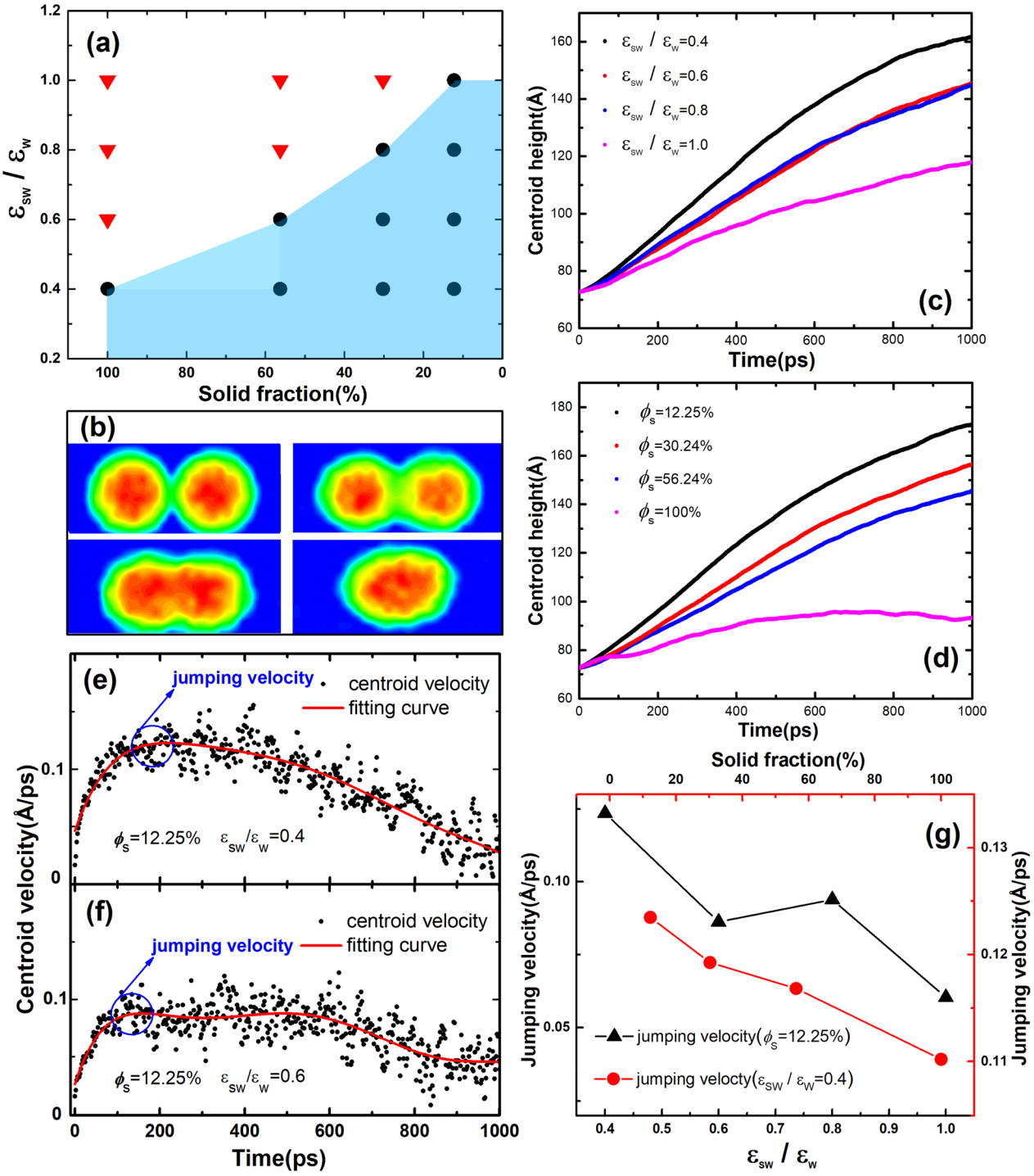

Figure 4. (a) Simulation results for 16 cases. Black points denote the successful induced jumping cases, and red triangles denote the failed jumping cases; the blue shaded area represents predictions of the successful jumping cases. (b) Density contours of droplets during coalescence process. (c) Effect of the surface wettability on the evolution of droplets centroid height (ϕ_s = 12.25%). (d) Effect of the solid fraction on the evolution of droplets centroid height ($\varepsilon_{sw}/\varepsilon_w$ = 0.6). (e, f) Evolution of the instantaneous vertical velocity for droplet centroid on different surfaces. (g) Dependency of the jumping velocity with respect to the solid fraction and the surface wettability intensity.

In summary, the coalescence process of two same-sized nanodroplets was studied numerically using the molecular dynamics simulation, and we investigated the effects of solid fraction and surface wettability intensity on the coalescence-induced jumping. It is found that coalescence-induced jumping exists in nanoscale droplets, which differs from previous theoretical predictions. The nanodroplets undergo coalescence in the inertially limited-viscous regime with liquid bridge radius R_b that evolves with time t as $R_b(t) \sim 0.9t^{0.4}$. The attraction force between the surface and water molecules is critical to this coalescence-induced jumping. The coalescence-induced jumping is more likely to happen on those surfaces with lower attraction force. Surface wettability intensity and solid fraction play a remarkable role in the adjustment of the attraction force, and this attraction force reduces along with decreasing surface wettability intensity and solid fraction. We believe these

DOI: 10.1021/acs.jpclett.7b02939
J. Phys. Chem. Lett. 2018, 9, 13−18

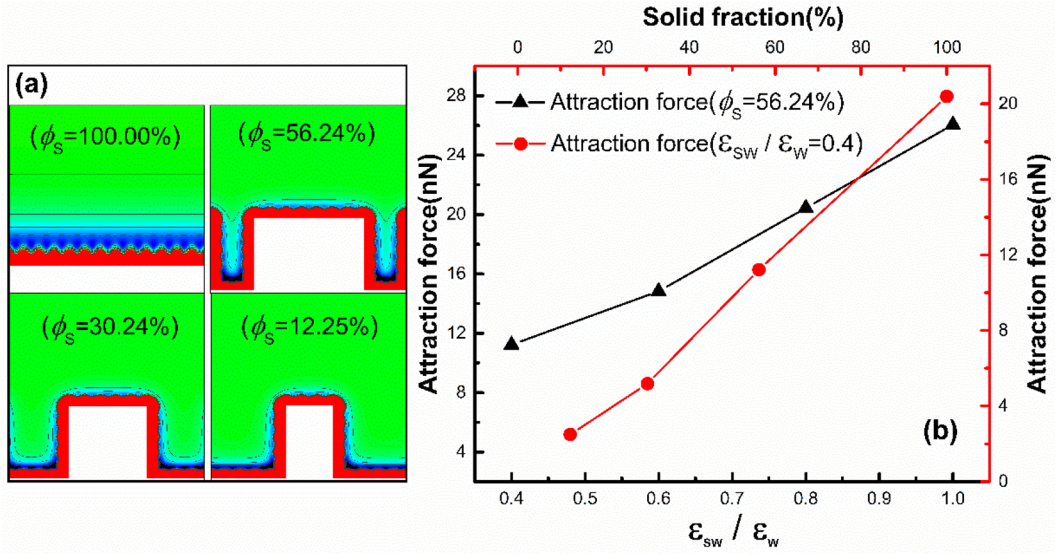

Figure 5. (a) Equipotential curves of interaction force between water molecules and substrates in the same unit area. (b) Dependency of the attraction force computed values with respect to the solid fraction and the surface wettability intensity.

findings are conducive to the design of self-cleaning surfaces with nanostructures and provide a fundamental insight into the improvement of hydrodynamics behavior in merged nanodroplets.

■ ASSOCIATED CONTENT

Supporting Information

The Supporting Information is available free of charge on the ACS Publications website at DOI: 10.1021/acs.jpclett.7b02939.

Simulation details, the contact angle of nanodroplets on smooth surfaces with different wettability intensity and energy conversation efficiency (PDF).

■ AUTHOR INFORMATION

Corresponding Authors

*E-mail: w_liu@hust.edu.cn.
*E-mail: zcliu@hust.edu.cn.

ORCID

Zhichun Liu: 0000-0001-9645-3052

Notes

The authors declare no competing financial interest.

■ ACKNOWLEDGMENTS

This project was supported by the National Natural Science Foundation of China (Nos. 51736004 and 51776079). The study was performed at the National Supercomputer Center in Tianjin, and the calculations were performed on TianHe-1(A).

■ REFERENCES

(1) Yoshimitsu, Z.; Nakajima, A.; Watanabe, T.; Hashimoto, K. Effects of surface structure on the hydrophobicity and sliding behavior of water droplets. *Langmuir* **2002**, *18*, 5818−5822.
(2) Hong, X.; Gao, X.; Jiang, L. Application of superhydrophobic surface with high adhesive force in no lost transport of superparamagnetic microdroplet. *J. Am. Chem. Soc.* **2007**, *129*, 1478−1479.
(3) Xiao, F.; Yuan, S.; Liang, B.; Li, G.; Pehkonen, S. O.; Zhang, T. Superhydrophobic CuO nanoneedle-covered copper surfaces for anticorrosion. *J. Mater. Chem. A* **2015**, *3*, 4374−4388.
(4) Miljkovic, N.; Enright, R.; Wang, E. N. Effect of droplet morphology on growth dynamics and heat transfer during condensation on superhydrophobic nanostructured surfaces. *ACS Nano* **2012**, *6*, 1776−1785.
(5) Gao, X.; Yao, X.; Jiang, L. Effects of rugged nanoprotrusions on the surface hydrophobicity and water adhesion of anisotropic micropatterns. *Langmuir* **2007**, *23*, 4886−4891.
(6) Liu, Y.; Moevius, L.; Xu, X.; Qian, T.; Yeomans, J. M.; Wang, Z. Pancake bouncing on superhydrophobic surfaces. *Nat. Phys.* **2014**, *10*, 515−519.
(7) Wen, R.; Li, Q.; Wang, W.; Latour, B.; Li, C. H.; Li, C.; Lee, Y. C.; Yang, R. Enhanced Bubble Nucleation and Liquid Rewetting for Highly Efficient Boiling Heat Transfer on Two-Level Hierarchical Surfaces with Patterned Copper Nanowire Arrays. *Nano Energy* **2017**, *38*, 59−65.
(8) Mouterde, T.; Lehoucq, G.; Xavier, S.; Checco, A.; Black, C. T.; Rahman, A.; Midavaine, T.; Clanet, C.; Quere, D. Antifogging abilities of model nanotextures. *Nat. Mater.* **2017**, *16*, 658−663.
(9) Gao, S.; Liao, Q.; Liu, W.; Liu, Z. Effects of solid fraction on droplet wetting and vapor condensation: a molecular dynamic simulation study. *Langmuir* **2017**, *33*, 12379−12388.
(10) Boreyko, J. B.; Chen, C. H. Self-propelled dropwise condensate on superhydrophobic surfaces. *Phys. Rev. Lett.* **2009**, *103*, 184501.
(11) Xu, Q.; Li, J.; Tian, J.; Zhu, J.; Gao, X. Energy-effective frost-free coatings based on superhydrophobic aligned nanocones. *ACS Appl. Mater. Interfaces* **2014**, *6*, 8976−8980.
(12) Zhang, Q.; He, M.; Chen, J.; Wang, J.; Song, Y.; Jiang, L. Anti-icing surfaces based on enhanced self-propelled jumping of condensed water microdroplets. *Chem. Commun.* **2013**, *49*, 4516−4518.
(13) Miljkovic, N.; Preston, D. J.; Enright, R.; Wang, E. N. Electrostatic charging of jumping droplets. *Nat. Commun.* **2013**, *4*, 2517.
(14) Miljkovic, N.; Enright, R.; Nam, Y.; Lopez, K.; Dou, N.; Sack, J.; Wang, E. N. Jumping-droplet-enhanced condensation on scalable superhydrophobic nanostructured surfaces. *Nano Lett.* **2013**, *13*, 179−187.
(15) Zhu, J.; Luo, Y.; Tian, J.; Li, J.; Gao, X. Clustered ribbed-nanoneedle structured copper surfaces with high-efficiency dropwise condensation heat transfer performance. *ACS Appl. Mater. Interfaces* **2015**, *7*, 10660−10665.
(16) Hou, Y.; Yu, M.; Chen, X.; Wang, Z.; Yao, S. Recurrent filmwise and dropwise condensation on a beetle mimetic surface. *ACS Nano* **2015**, *9*, 71−81.
(17) Chen, X.; Wu, J.; Ma, R.; Hua, M.; Koratkar, N.; Yao, S.; Wang, Z. Nanograssed Micropyramidal Architectures for Continuous Dropwise Condensation. *Adv. Funct. Mater.* **2011**, *21*, 4617−4623.

DOI: 10.1021/acs.jpclett.7b02939
J. Phys. Chem. Lett. 2018, 9, 13−18

(18) Wen, R.; Li, Q.; Wu, J.; Wu, G.; Wang, W.; Chen, Y.; Ma, X.; Zhao, D.; Yang, R. Hydrophobic copper nanowires for enhancing condensation heat transfer. *Nano Energy* **2017**, *33*, 177−183.
(19) Enright, R.; Miljkovic, N.; Sprittles, J.; Nolan, K.; Mitchell, R.; Wang, E. N. How coalescing droplets jump. *ACS Nano* **2014**, *8*, 10352−10362.
(20) Tian, J.; Zhu, J.; Guo, H. Y.; Li, J.; Feng, X. Q.; Gao, X. Efficient Self-Propelling of Small-Scale Condensed Microdrops by Closely Packed ZnO Nanoneedles. *J. Phys. Chem. Lett.* **2014**, *5*, 2084−2088.
(21) Li, H.; Yang, W.; Aili, A.; Zhang, T. Insights into the Impact of Surface Hydrophobicity on Droplet Coalescence and Jumping Dynamics. *Langmuir* **2017**, *33*, 8574−8581.
(22) Chen, X.; Patel, R. S.; Weibel, J. A.; Garimella, S. V. Coalescence-Induced Jumping of Multiple Condensate Droplets on Hierarchical Superhydrophobic Surfaces. *Sci. Rep.* **2016**, *6*, 18649.
(23) Wang, F.; Yang, F.; Zhao, Y. Size effect on the coalescence-induced self-propelled droplet. *Appl. Phys. Lett.* **2011**, *98*, 053112.
(24) Liu, F.; Ghigliotti, G.; Feng, J. J.; Chen, C. Numerical simulations of self-propelled jumping upon drop coalescence on non-wetting surfaces. *J. Fluid Mech.* **2014**, *752*, 39−65.
(25) Farokhirad, S.; Mohammadi Shad, M.; Lee, T. Coalescence-induced jumping of immersed and suspended droplets on micro-structured substrates. *Eur. J. Comput. Mech.* **2017**, *26*, 1−19.
(26) Mulroe, M. D.; Srijanto, B. R.; Ahmadi, S. F.; Collier, C. P.; Boreyko, J. B. Tuning Superhydrophobic Nanostructures To Enhance Jumping-Droplet Condensation. *ACS Nano* **2017**, *11*, 8499−8510.
(27) Cha, H.; Xu, C.; Sotelo, J.; Chun, J. M.; Yokoyama, Y.; Enright, R.; Miljkovic, N. Coalescence-induced nanodroplet jumping. *Phys. Rev. Fluids* **2016**, *1*, 064102.
(28) Liang, Z.; Keblinski, P. Coalescence-induced jumping of nanoscale droplets on super-hydrophobic surfaces. *Appl. Phys. Lett.* **2015**, *107*, 143105.
(29) Liu, T. Q.; Sun, W.; Sun, X. Y.; Ai, H. R. Mechanism study of condensed drops jumping on super-hydrophobic surfaces. *Colloids Surf., A* **2012**, *414*, 366−374.
(30) Liu, X.; Cheng, P. 3D multiphase lattice Boltzmann simulations for morphological effects on self-propelled jumping of droplets on textured superhydrophobic surfaces. *Int. Commun. Heat Mass Transfer* **2015**, *64*, 7−13.
(31) Fezzaa, K.; Wang, Y. Ultrafast x-ray phase-contrast imaging of the initial coalescence phase of two water droplets. *Phys. Rev. Lett.* **2008**, *100*, 104501.
(32) Yao, W.; Maris, H. J.; Pennington, P.; Seidel, G. M. Coalescence of viscous liquid drops. *Phys. Rev. E* **2005**, *71*, 016309.
(33) Paulsen, J. D.; Burton, J. C.; Nagel, S. R.; Appathurai, S.; Harris, M. T.; Basaran, O. A. The inexorable resistance of inertia determines the initial regime of drop coalescence. *Proc. Natl. Acad. Sci. U. S. A.* **2012**, *109*, 6857−6861.

DOI: 10.1021/acs.jpclett.7b02939
J. Phys. Chem. Lett. 2018, 9, 13−18